Effect of He-appm/DPA ratio on the damage microstructure of tungsten

R.W. Harrison, H. Amari, G. Greaves, J.A. Hinks and S.E. Donnelly

School of Computing and Engineering, University of Huddersfield, Huddersfield, HD1 3DH

Abstract

In-situ ion irradiation and transmission electron microscopy has been used to examine the effects of the He appm to DPA ratio, temperature and dose on the damage structure of tungsten (W). Irradiations were performed with 15 or 60 keV He[+] ions, achieving He-appm/displacements per atom (DPA) ratios of ~40,000 and ~2000, respectively, at temperatures between 500 and 1000°C to a dose of ~3 DPA. A high number of small dislocation loops with sizes around 5–20 nm and a He bubble lattice were observed for both He-appm/DPA ratios at 500°C with a bubble size ~1.5 nm. Using the ***g.b***=0 criterion the loops were characterised as ***b*** = ±1/2<111> type. At 750°C bubbles do not form an ordered array and are larger in size compared to the irradiations at 500°C, with a diameter of ~3 nm. Fewer dislocation loops were observed at this temperature and were also characterised to be ***b*** = ±1/2<111> type. At 1000°C, no dislocation loops were observed and bubbles grew as a function of fluence attributed to vacancy mobility being higher and vacancy clusters becoming mobile.

1 Introduction

Tungsten (W) is regarded as the primary candidate for use as a plasma facing material in the divertor of the ITER and DEMO fusion reactors due to its high melting temperature (~3400°C), low sputter yield and high thermal conductivity (~170 W.m^{-1}.K^{-1} at room temperature)[1]. However, during service, the divertor will be exposed to high heat fluxes, radiation damage from 14.1 MeV neutrons and He injection from the plasma as well as He production from (n,α) reactions. The production of He from (n,α) reactions in W is low, with only around 5 atomic parts per million (appm) He being produced after 2 full power years in the DEMO reactor [2] resulting in a He-appm per displacement per atom (DPA) ratio of ~0.6. However, towards the surface the He-appm/DPA ratio will rise to 1000s from He injection from the plasma.

Tanno *et al.* [3], [4] report the formation of a void lattice in fast neutron irradiated W in the JOYO reactor at 750°C at 1.54 DPA (He-appm/DPA ~0.6). The authors report the formation of small voids of around 5 nm in samples irradiated at 400 and 750°C. Fukuda *et al.* [5] observed void formation only at higher (800°C) temperatures, however, these irradiations were performed in HFIR under thermal neutron irradiation which may be the cause of the difference in temperature that voids were observed at compared with Tanno *et al.* Yi *et al.* [6], [7] examined the effect of self-ion irradiation on the damage microstructure of W using 2 MeV W$^+$ to fluences of $3.7×10^{13}$ and $2.5×10^{15}$ W.cm^{-2} to a total of 3 DPA at temperatures of 300, 500 and 750°C (He-appm/DPA = 0). Small dislocation loops, mainly of ***b*** = ±1/2<111> type which consisted of an equal amount of vacancy and interstitial type loops, a minority of <100> type loops were also observed.

Much work has focused on the effect of low energy He ions (< 5 keV, He-appm/DPA >1000s) on W to mimic the plasma-W interaction [8]–[15]. This results in the formation of so called 'surface fuzz' which leads to a reduction in effective thermal conductivity and increase in embrittlement leading to issues with surface melting and plasma erosion.

The effects of how the He-appm to DPA ratio effect the damage microstructure of W in the literature are often difficult to extract and compare due to variations in the experimental conditions between studies. This work aims to study the damage microstructure of W using He$^+$ ion irradiation to concomitantly impart damage and implant He. Using the *in-situ* ion irradiation technique with He$^+$ the He-appm/DPA ratio can be altered simply by changing the energy of the incident He$^+$ beam, by increasing the beam energy the amount of He implantation into a transmission electron microscope

(TEM) foil of around 50–60 nm thickness will decrease, reducing the He-appm/DPA ratio. By altering the He-appm/DPA ratio, temperature and total fluence (dose), we will be able to generate a consistent dataset of how these 3 parameters affect the damage microstructure of W.

2 Experimental

Samples of W were prepared by punching 3 mm discs from foil (Alfa-Aesar, 99.95 wt-%, main impurity C 0.003 wt%). The discs were then annealed at 1400°C for 2 hours under vacuum (0.1 Pa) to remove any pre-existing effects from cold working. After annealing the discs were electropolished with 0.5 wt-% NaOH solution with a Tenupol-5 at room temperature. Samples were washed in three separate baths of CH_3OH to remove any residue from the electrolyte.

In-situ ion irradiation was performed using the Microscope and Ion Accelerator for Materials Investigation facility (MIAMI-1) consisting of a JEOL JEM-2000FX operated at 200 kV were the electron beam was incident to the sample normal and the ion beam was 30° to the sample normal. Post-irradiation examination (PIE) was also performed with a JEOL JEM-3010 operated at 300 kV.

Damage and He implantation were calculated using the *Stopping Range of Ions in Matter* (SRIM) Monte Carlo computer code [16]. DPA was calculated using the method proposed by Stoller *et al.* [17] using a displacement energy for W of 90 eV [18]. Samples were irradiated using 15 or 60 keV He^+ ions to achieve He-appm/DPA ratios of ~40,000 and ~2,000, respectively. The flux was set for each He^+ energy to keep the DPA rate constant at ~9×10^{-4} $DPA.s^{-1}$ with a flux of ~3.40×10^{13} and ~6.8×10^{13} $ions.cm^{-2}.s^{-1}$ for 15 and 60 keV, respectively. The difference in the rise of temperature induced from the ion beam was calculated to be 0.5-2.5°C for the 15 and 60 keV experiments respectively across the entire sample and so the difference in heating between the different fluxes is considered negligible. The effect of temperature was examined with irradiations performed at 500 and 750°C for both He-appm/DPA ratios and also 1000°C for the He-appm/DPA ratio of ~2000.

3 Results and Discussion

3.1 Damage microstructure with a He apppm/DPA ratio ~2000

Samples irradiated at 500°C showed the formation of small (<5 nm) loops which grew in number density but did not grow in size (Figure 1). It was observed that the loops appeared/disappeared randomly across the grains throughout the experiments and as such we did not observe a significant change in number density as a function of local changes in diffraction contrast. Figure 2 shows post irradiation two-beam bright field (BF) imaging of the dislocation loops after 3 DPA with the circled loops generating contrast when $g = \bar{1}10$ and 020 were excited but no contrast when $g = 12\bar{1}$ is excited, indicating they have a Burgers vector of $b = \pm1/2[\bar{1}11]$. He bubbles with a diameter of around 1.5 nm were observed to form a bubble lattice (Figure 3) which has been observed previously in W under He^+ irradiation at similar temperatures [19].
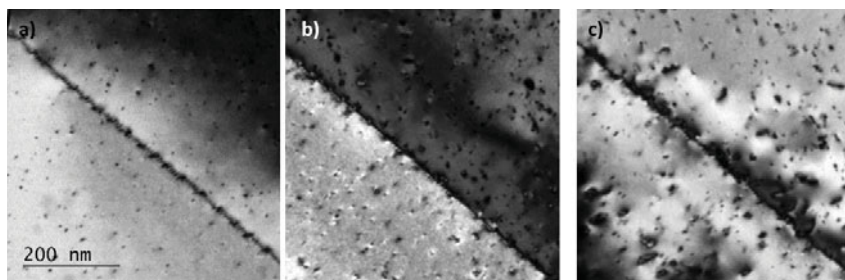

Figure 1. BF-TEM images of W sample irradiated at 500°C with 60 keV He^+ ions achieving a He appm/DPA ratio of ~2000 to: a) 1.0 DPA, b) 2.0 DPA and c) 3.0 DPA.
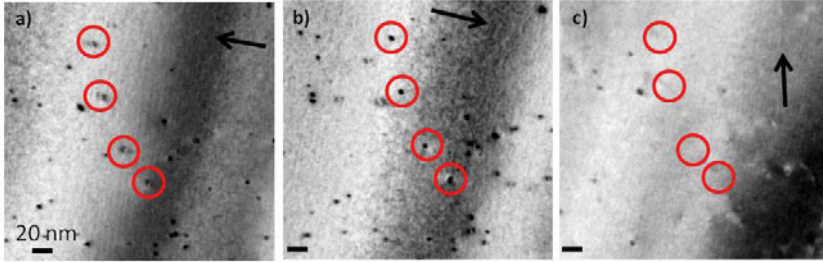
Figure 2. Two-beam TEM images of W sample irradiated at 500°C with 60 keV He$^+$ ions to 3 DPA with a He appm/DPA ratio of ~2000, arrows indicate excited g vector, a) $g = \bar{1}10$, b) $g = 1\bar{1}0$ and c) $g = 12\bar{1}$.
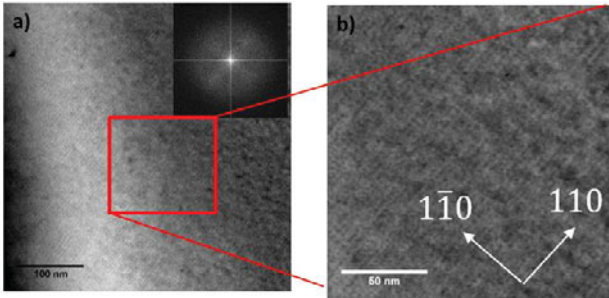

Figure 3. a) BF-TEM image of sample irradiated at 500°C with 60 keV He$^+$ ions to 3 DPA with a He appm/DPA ratio of ~2000 taken at +0.76 μm overfocus showing bubble lattice formed. Inset shows reduced fast Fourier transform (FFT) of image showing a 3D ordering of the bubbles and b) shows enlarged area within square in a
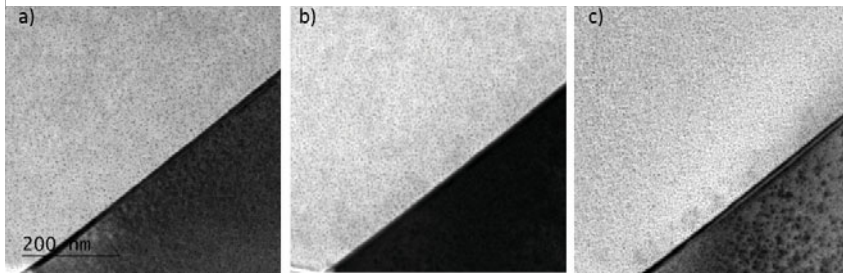

Figure 4. BF-TEM images of bubbles in W sample irradiated at 750°C with 60 keV He$^+$ ions, achieving a He appm/DPA ratio of ~2,000 to: a) 1.0 DPA, b) 2.0 DPA and c) 3.0 DPA. Images taken at +3.1μm focus with bubbles appearing as dark circles.

Increasing the irradiation temperature to 750°C revealed a largely different microstructure. In this case, larger bubbles of around 3 nm in diameter appeared and grew in number density as a function of fluence. Figure 4 shows the evolution of the microstructure, bubble size and density as a function of DPA using 60 keV He$^+$ ions, achieving a He-appm/DPA ratio of ~2000 at 750°C to 3 DPA. Post-irradiation analysis revealed the presence of small (< 5 nm) dislocation loops shown in Figure 5, it can be seen that the loops were of $\boldsymbol{b} = \pm 1/2\langle 111\rangle$ type. Monovacancy migration in W has an activation energy of 1.7 eV and becomes important at temperatures above 0.15 of the melting temperature (T_m)

[20]. At the irradiation temperature of 750°C, larger bubble formation compared to the 500°C irradiation is evidence for a higher mobility of vacancies.

Irradiations at 1000°C revealed a damage microstructure than consisted solely of He bubbles and no loops shown in Figure 6. The bubbles grew in size, from around 4 to 7 nm in diameter from 0.25 to 1.0 DPA respectively (fluence $=1\times10^{17}$ ions.cm^{-2}).
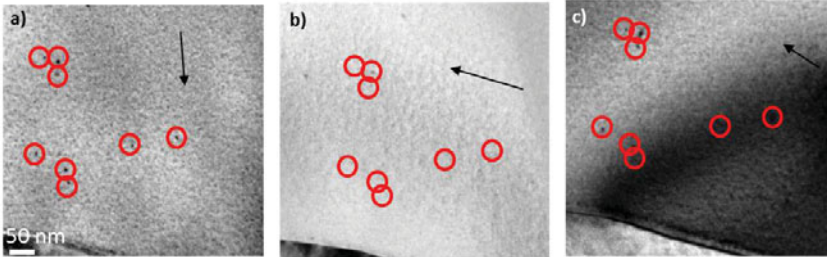

Figure 5. Two-beam TEM taken at –304 nm underfocus, images of sample irradiated at 750 °C using 60 keV He$^+$ ions to achieve a He appm/DPA ratio ~2,000 to 3.0 DPA, arrows indicate *g* vector excited a) $\overline{1}10$ b) $\overline{1}2\overline{1}$ and c) $0\overline{2}0$.
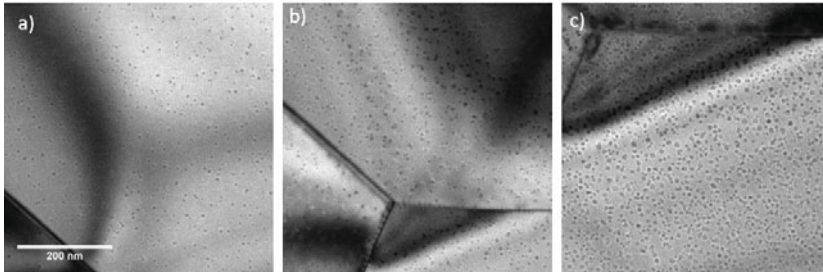

Figure 6. BF-TEM images of sample irradiated at 1000°C using 60 keV He ions to achieve a He appm/DPA ratio of ~2,000 , all images at +4.6 µm focus a) 0.25 DPA, b) 0.5 DPA and c) 1.0 DPA

A high temperature recovery stage in W is reported at around 0.31 T_m, ~850°C. However, the process behind this recovery stage is still a subject of debate and has been attributed to the migration of larger clusters and emission of monovacancies from clusters resulting in void coarsening [21]. Monovacancies will be very mobile at this temperature (0.35 T_m). Bubble coalescence was also observed with bubble growth resulting in agglomeration with other bubbles in close proximity and not via bubble migration.

3.2 Damage microstructure with a He-apppm/DPA ratio ~40,000

Samples irradiated at 500°C showed the formation of a bubble lattice with bubbles ~1.5 nm in diameter, similar to the sample irradiated with a He-appm/DPA ratio of ~2000. Figure 7 shows the evolution of the microstructure as a function of fluence. Figure 7a shows the presence of small (≤ 5 nm) dislocation loops and a bubble lattice is confirmed by the FFT inset in Figure 7a showing 4 lobes confirming 2D ordering in the image, however, as this is a transmission image it indicates the ordering will also be into the plane of the image, suggesting 3D ordering of bubbles. PIE revealed a range of dislocation loop sizes in the region of ~5–20 nm – larger than those seen in the lower He-appm/DPA ratio. Figure 8 shows post irradiation two-beam imaging of the dislocation loops after 3 DPA with the solid line circled loops showing contrast when $g = 020$ and $\overline{1}2\overline{1}$ and no contrast when $g = 21\overline{1}$ was excited indicating they have a Burgers vector of $b = \pm1/2[1\overline{1}1]$. The loops circled with a dashed line were determined to also be $b = \pm1/2<111>$ type dislocation loops with a Burgers vector of
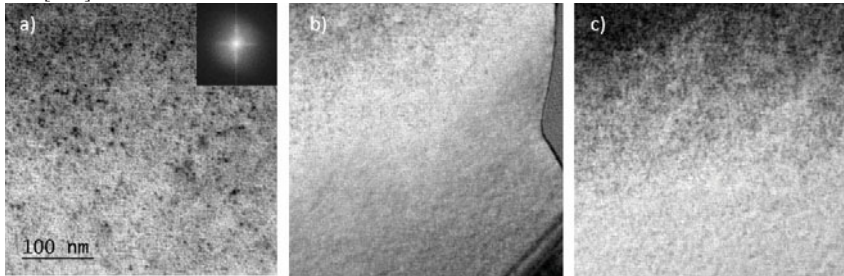
$\pm 1/2[\bar{1}11]$.

Figure 7. BF-TEM images of sample irradiated at 500°C with 15 keV He$^+$ ions to achieve a He-appm/DPA ratio of ~40,000. Images taken with +3.1 µm overfocus a) 1.0 DPA (inset is FFT of image showing 4 lobes indicative of 3D ordering), b) 2.0 DPA and c) 3.0 DPA.
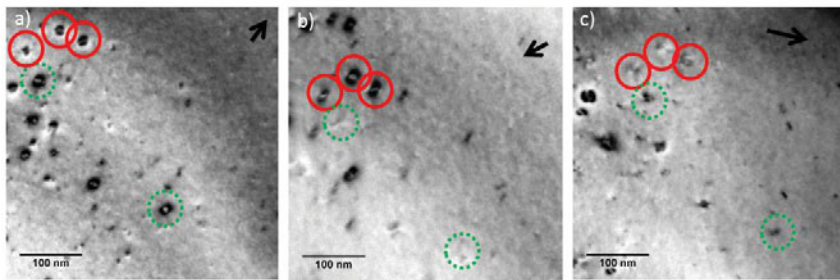

Figure 8. Two-beam TEM images taken close to focus of sample irradiated at 500°C with 15 keV He$^+$ ions to achieve a He-appm/DPA ratio of ~40,000 to 3.0 DPA: a) $g = 020$, b) $g = 21\bar{1}$, and c) $g = \bar{1}2\bar{1}$.

Increasing the irradiation temperature to 750°C resulted in larger bubbles, ~3 nm in diameter which grew in number density as a function of fluence but remained around constant in size, similar to the samples irradiated with a He-appm/DPA ratio ~2,000. Figure 9 shows the evolution of the microstructure a function of DPA. At the irradiation temperature of 750°C, a larger average bubble size is evidence for a higher mobility of vacancies compared to the irradiation at 500°C.
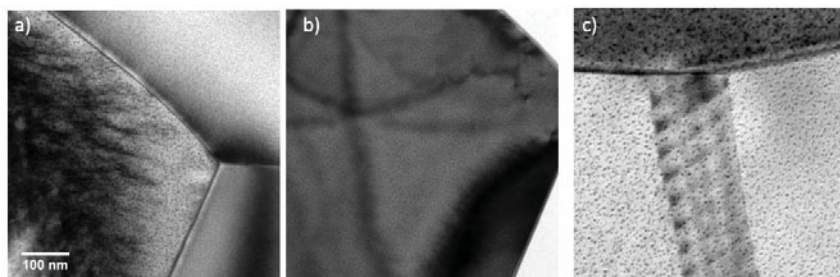

Figure 9. BF-TEM images of W sample irradiated at 750°C: a) 0.7 DPA, b) 1.5 DPA and c) 2.2 DPA. All images taken with +3.1 µm underfocus.

4 Conclusions

W samples were observed *in situ* via TEM whilst being irradiated using He$^+$ ions at 15 or 60 keV achieving a He-appm/DPA ratio of ~40,000 or ~2000, respectively, at temperatures between 500 and 1000°C to a dose of ~3 DPA. A high number of small dislocation loops with sizes around 5–10 nm and a He bubble lattice were observed for both He-appm/DPA ratios at 500°C with a bubble size ~1.5 nm. Using the $g.b=0$ criterion, the loops were characterised as $b = \pm1/2<111>$ type and it is assumed that with vacancies forming the bubble lattice it is likely the loops are interstitial in nature. At 750°C bubbles do not form an ordered array and are larger in size compared to the irradiations at 500°C, with a diameter of ~3 nm. A lower density of dislocation loops were observed at this temperature and were also characterised to be $b = \pm1/2<111>$ type loops. At 1000°C no dislocation loops are observed and bubbles grow as a function of fluence from ~4 to 7 nm in diameter up to 1.0 DPA (fluence ~1×10^{17} ions.cm^{-2}). This is attributed to vacancy mobility being higher and larger vacancy clusters becoming mobile at temperatures above 0.31 T_m (stage V recovery step) as well as becoming unstable via dissociation into monovacancies providing a high flux of vacancies for growth as well as by bubble coalescence.

Acknowledgments

References

[1]   H. Bolt, V. Barabash, W. Krauss, J. Linke, R. Neu, S. Suzuki, N. Yoshida, and A. U. Team, "Materials for the plasma-facing components of fusion reactors."

[2]   M. R. Gilbert, S. L. Dudarev, S. Zheng, L. W. Packer, and J.-C. Sublet, "An integrated model for materials in a fusion power plant: transmutation, gas production, and helium embrittlement under neutron irradiation," *Nucl. Fusion*, vol. 52, no. 8, p. 083019, 2012.

[3]   T. Tanno, A. Hasegawa, J.-C. He, M. Fujiwara, S. Nogami, M. Satou, T. Shishido, and K. Abe, "Effects of Transmutation Elements on Neutron Irradiation Hardening of Tungsten," *Mater. Trans.*, vol. 48, no. 9, pp. 2399–2402, 2007.

[4]   T. Tanno, a. Hasegawa, J. C. He, M. Fujiwara, M. Satou, S. Nogami, K. Abe, and T. Shishido, "Effects of transmutation elements on the microstructural evolution and electrical resistivity of neutron-irradiated tungsten," *J. Nucl. Mater.*, vol. 386–388, no. 2009, pp. 218–221, 2009.

[5]   M. Fukuda, K. Yabuuchi, S. Nogami, A. Hasegawa, and T. Tanaka, "Microstructural development of tungsten and tungsten–rhenium alloys due to neutron irradiation in HFIR," *J. Nucl. Mater.*, vol. 455, pp. 460–463, 2014.

[6]   X. Yi, M. L. Jenkins, M. Briceno, S. G. Roberts, Z. Zhou, and M. A. Kirk, "In-situ study of self-ion irradiation damage in W and W-5Re at 500°C," *Philos. Mag. A*, vol. 93, no. 14, pp. 1715–1738, 2012.

[7]   X. Yi, M. L. Jenkins, K. Hattar, P. D. Edmondson, and S. G. Roberts, "Characterisation of radiation damage in W and W-based alloys from 2 MeV self-ion near-bulk implantations," *Acta Mater.*, vol. 92, pp. 163–177, 2015.

[8]   O. El-Atwani, K. Hattar, J. A. Hinks, G. Greaves, S. S. Harilal, and A. Hassanein, "Helium bubble formation in ultrafine and nanocrystalline tungsten under different extreme conditions," *J. Nucl. Mater.*, vol. 458, pp. 216–223, Mar. 2015.

[9]   O. El-Atwani, J. A. Hinks, G. Greaves, S. Gonderman, T. Qiu, M. Efe, and J. P. Allain, "In-situ TEM observation of the response of ultrafine- and nanocrystalline-grained tungsten to extreme irradiation environments.," *Sci. Rep.*, vol. 4, p. 4716, 2014.

[10] H. Iwakiri, K. Yasunaga, K. Morishita, and N. Yoshida, "Microstructure evolution in tungsten during low-energy helium ion irradiation."

[11] H. T. Lee, A. A. Haasz, J. W. Davis, R. G. Macaulay-Newcombe, D. G. Whyte, and G. M.

Wright, "Hydrogen and helium trapping in tungsten under simultaneous irradiations."

[12] M. Miyamoto, S. Mikami, H. Nagashima, N. Iijima, D. Nishijima, R. P. Doerner, N. Yoshida, H. Watanabe, Y. Ueda, and A. Sagara, "Systematic investigation of the formation behavior of helium bubbles in tungsten," *J. Nucl. Mater.*, vol. 463, pp. 333–336, Aug. 2015.

[13] D. Nishijima, M. . Ye, N. Ohno, and S. Takamura, "Formation mechanism of bubbles and holes on tungsten surface with low-energy and high-flux helium plasma irradiation in NAGDIS-II," *J. Nucl. Mater.*, vol. 329–333, pp. 1029–1033, Aug. 2004.

[14] Y. Ueda, M. Fukumoto, J. Yoshida, Y. Ohtsuka, R. Akiyoshi, H. Iwakiri, and N. Yoshida, "Simultaneous irradiation effects of hydrogen and helium ions on tungsten," *J. Nucl. Mater.*, vol. 386–388, pp. 725–728.

[15] N. Yoshida, H. Iwakiri, K. Tokunaga, and T. Baba, "Impact of low energy helium irradiation on plasma facing metals."

[16] J. F. Ziegler, "Stopping of energetic light ions in elemental matter," *J. Appl. Phys.*, vol. 85, no. 3, p. 1249, 1999.

[17] R. E. Stoller, M. B. Toloczko, G. S. Was, A. G. Certain, S. Dwaraknath, and F. A. Garner, "On the use of SRIM for computing radiation damage exposure," *Nucl. Instruments Methods Phys. Res. Sect. B Beam Interact. with Mater. Atoms*, vol. 310, pp. 75–80, 2013.

[18] A. E521, "Standard Practice for Neutron Radiation Damage Simulation by Charged-Particle," *Annu. B. ASTM Stand.*, vol. 12.02, no. Reapproved, pp. 1–21, 2009.

[19] P. B. Johnson and D. J. Mazey, "Gas-bubble superlattice formation in bcc metals," *J. Nucl. Mater.*, vol. 218, no. 3, pp. 273–288, Mar. 1995.

[20] F. Ferroni, X. Yi, K. Arakawa, S. P. Fitzgerald, P. D. Edmondson, and S. G. Roberts, "High temperature annealing of ion irradiated tungsten," *Acta Mater.*, vol. 90, pp. 380–393, 2015.

[21] D. R. M. and X. Y. and M. A. K. and S. L. Dudarev, "Elastic trapping of dislocation loops in cascades in ion-irradiated tungsten foils," *J. Phys. Condens. Matter*, vol. 26, no. 37, p. 375701, 2014.